

# Operational Modal Analysis on Structures with Rotating Parts

**N-J. Jacobsen**

Brüel & Kjær Sound & Vibration Measurement A/S

Skodsborgvej 307, DK-2850 Nærum, Denmark

e-mail: [njjacobsen@bksv.com](mailto:njjacobsen@bksv.com)

**P. Andersen**

Structural Vibration Solutions A/S

NOVI Science Park, Niels Jerners Vej 10, DK-9220 Aalborg East, Denmark

## Abstract

Operational Modal Analysis was originally invented for vibration analysis on civil engineering structures exposed to ambient excitation being purely stochastic and broadband in nature. When performing Operational Modal Analysis on civil or mechanical engineering structures with dominating rotating parts, the original algorithms are often inadequate in providing accurate results due to deterministic excitation.

This paper describes recently developed algorithms allowing Operational Modal Analysis to be performed on structures, where a significant part of the vibration is originating from the rotating parts. This includes Fast Kurtosis Checking, Enhanced Kurtosis Checking and the Curve-fitting Frequency Domain Decomposition technique. In addition, practical measurement considerations concerning dynamic range and time recording length are discussed.

The applicability of the algorithms is assessed for cases within civil and mechanical engineering.

## 1 Introduction

The algorithms used in Operational Modal Analysis assume that the input forces to the structure under test are stochastic in nature. However, the excitation often consist of strong harmonic components (deterministic signals) superimposed on the stochastic broadband excitation. As the input forces are not measured in Operational Modal Analysis, attention must be paid to identify and separate the harmonic components from the structural modes and to reduce their influence on the extracted modal parameters. As described in Jacobsen [1], the consequences of having stochastic signals superimposed by harmonic components can be quite severe and can significantly bias the modal parameters obtained or even prohibit the extraction of the structural modes.

In Jacobsen [1] various easy-to-use methods for identifying harmonic components and structural modes were also investigated. This included the Short Time Fourier Transform (STFT), Singular Value Decomposition (SVD), Visual Mode Shape Comparison, Modal Assurance Criterion (MAC), Stabilization Diagram and Probability Density Functions (PDFs). Despite being very powerful in the cases of well-separated structural modes and harmonic components, the methods were not very suitable for a robust automated method for separating closely-coupled structural modes and harmonic components.

In Jacobsen et al. [2] a robust automated harmonic indicator based on kurtosis calculations was introduced. Harmonic components were suppressed by linear interpolation in the Single-Degree-Of-Freedom (SDOF) functions of the Enhanced Frequency Domain Decomposition (EFDD) technique, i.e. without using potentially destructive filtering. The method gave good results but could be optimized for computational efficiency and accuracy for harmonic components located exactly at the natural frequencies.

This paper presents a significantly faster version of the harmonic indicator called Fast Kurtosis Checking. Instead of checking the responses in every measurement channel at all frequencies, only selected channels and frequencies are investigated. Having detected the harmonic components, their influence are significantly reduced by applying a Curve-fitting Frequency Domain Decomposition (CFDD) technique giving a more accurate estimation of the natural frequencies and damping ratios than the EFDD technique. The applicability of the new combined approach is discussed and applied to two real cases within mechanical engineering and civil engineering – a ship structure and a gravity dam.

Furthermore, practical measurement considerations concerning dynamic range and time recording length are discussed.

## 2 Identification of Harmonic Components

### 2.1 Extended Kurtosis Checking

In Jacobsen et al. [2] an Extended Kurtosis Checking method was described and shown to be a robust harmonic indicator. It was based on various applications of kurtosis calculations. The kurtosis  $\gamma$  of a stochastic variable  $x$  provides a measure of how peaked the probability density function of  $x$  is. The kurtosis is defined as the fourth central moment of the stochastic variable normalized with respect to the standard deviation  $\sigma$ :

$$\gamma(x|\mu, \sigma) = \frac{E[(x - \mu)^4]}{\sigma^4} \quad (1)$$

where  $\mu$  is the mean value of  $x$  and  $E$  is denoting the expectation value.

The output of the Extended Kurtosis Checking method is a frequency dependent Harmonic Indicator  $H_j$  returning the value 1 in case of a harmonic component and otherwise 0. The steps in the automated Extended Kurtosis Checking method are roughly as follows:

1. Each measurement channel  $y_i$  is normalized to zero mean and unit variance.
2. For all frequencies  $f_j$  a narrow bandpass filtering of  $y_i$  around  $f_j$  is performed.
3. The Kurtosis  $\gamma_{,i}$  for the filtered signal  $y_i$  around  $f_j$  is calculated.
4. For each frequency  $f_j$ , the mean of the Kurtosis  $\gamma_j$  is calculated across all the measurement channels.
5. The median  $m$  of the Kurtosis of all frequencies is calculated. If the signal is purely Gaussian distributed this robust measure for the mean will theoretically be 3.
6. For each frequency  $f_j$  the deviation of the Kurtosis  $\gamma_j$  from the median  $m$  is calculated. For large deviations, the signals at  $f_j$  can be characterized as outliers and must be excluded in the estimation of the SDOF functions. Hence the harmonic indicator  $H_j$  is set equal to 1. Otherwise  $H_j$  is set equal to 0.
7. The harmonic indicator  $H_j$  is automatically plotted as vertical lines in the SVD plot of the response spectral density matrix.

Figure 1 shows the result of the Extended Kurtosis Check method applied to the responses of an aluminum plate structure excited with randomly spaced broadband stochastic excitation and a single-point sinusoidal signal at 374 Hz with 2<sup>nd</sup> and 4<sup>th</sup> harmonics at 748 Hz and 1496 Hz, respectively. The harmonic components are clearly found and indicated as vertical lines.

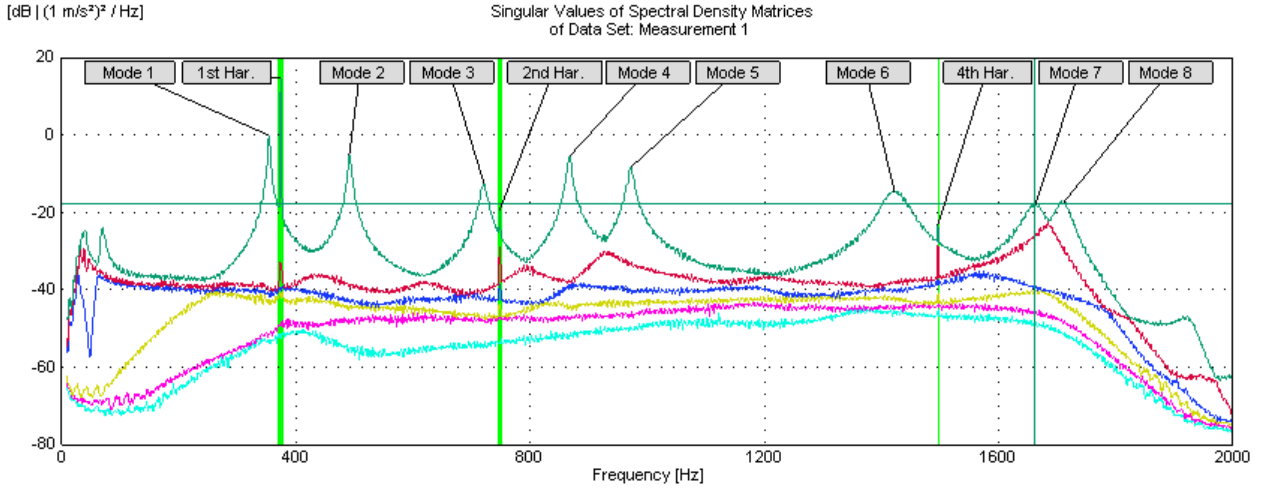


Figure 1. Indication of structural modes and harmonic components in the SVD plot with 6 projection channels. Harmonic components at 374 Hz, 748 Hz and 1496 Hz (vertical green lines).

## 2.2 Fast Kurtosis Checking

The Extended Kurtosis Checking method is computational intensive in case of many frequency lines and measurement channels. In Andersen et al. [3] an improved method called Fast Kurtosis Checking was proposed using fewer measurement channels and frequency lines.

### 2.2.1 Reducing the Number of Measurement Channels

The spectral density matrix  $G_{yy}(f)$  of the measured responses typically consist of many more rows and columns than there are structural modes. Many of the rows and columns are linear dependent resulting in a rank deficiency of the spectral matrix  $G_{yy}(f)$ . Consequently it is not necessary to include all of the measurement channels ( $n_y$ ) in the harmonic indicator algorithm. The subset to be used is called the projection channels and the number of projection channels is denoted  $n_p$ . Selection of the projection channels is based on calculating the correlation coefficients  $C_{ij}$  between the measurement channels  $y(t)$ :

$$C_{ij}^2 = \frac{E[(y_i(t)y_j(t))^2]}{E[y_i(t)y_i(t)] E[y_j(t)y_j(t)]} \quad (2)$$

The projection channels are automatically found using the following procedure:

- 1a. If the test is performed in multiple data sets, the reference channels are used as projection channels. These channels correlate most with the other channels, since they are present in all data sets
- 1b. If the test is performed in a single data set the channel  $i$  that correlates most with the other channels is used. This channel most likely contains maximum physical information. Channel  $i$  is found, where the function  $W_i$  is at maximum:

$$W_i = \sum_{j=1}^n |C_{ij}| \quad j \neq i, i = 1, \dots, n \quad , n: \text{ number of measurement channels} \quad (3)$$

2. Find the channel that correlates the least with all previous found projection channels. This channel will most likely bring most new information

3. Discard channel if too low correlation as it might be due to faulty or incorrectly mounted transducer
4. Repeat step 2 and 3 until all required projection channels are found

The number of projection channels required can be found by applying the Singular Value Decomposition (SVD) technique to the spectral densities matrices  $G_{yp}(f)$ :

$$USV^H = G_{yp}(f) \quad (4)$$

where index  $y$  indicate the measurement vector  $y(t)$  and  $p$  the projection channel. The matrices  $G_{yp}(f)$  and  $S$  both have dimension  $n_y \times n_p$ .  $S$  is a diagonal matrix consisting of  $n_p$  singular values.

By plotting the singular values at every frequency for all projection channels, all modes will be revealed. If the lower curve approximates a horizontal line over the frequency range of interest, and the other curves show good mode separation, then the number of projection channels is optimal as additional projection channels will not add any new information. Otherwise more or less projection channels should be used.

Figure 2 shows the aluminum plate example from Figure 1 without sinusoidal excitation. Too many channels have clearly been selected as projection channels. Figure 3 shows a more appropriate choice.

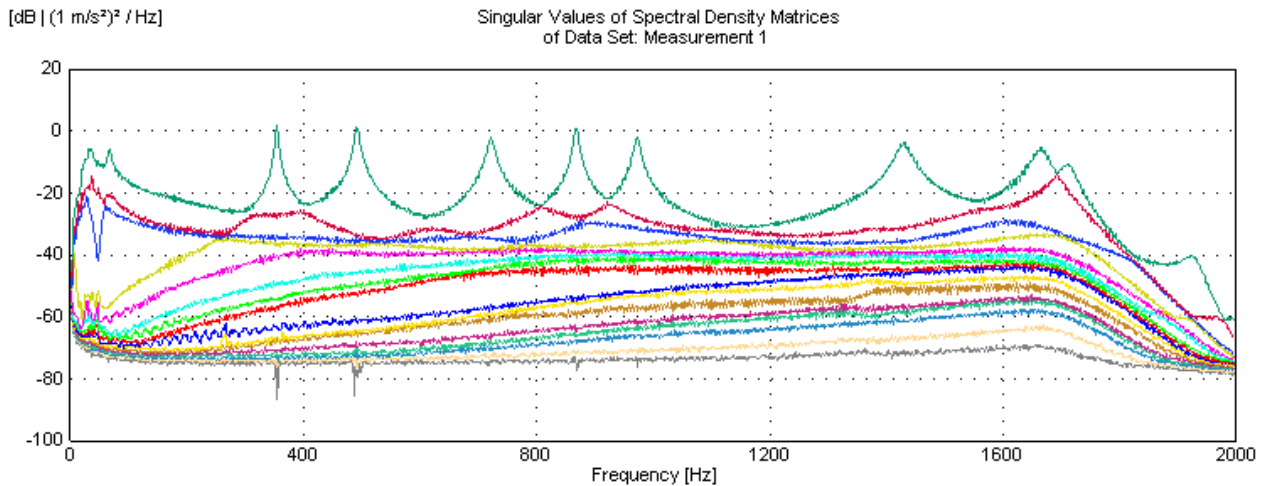


Figure 2. Example with 16 projection channels resulting in 16 singular value curves. All the lower curves are basically horizontal indicating a substantial amount of redundant information at all frequencies.

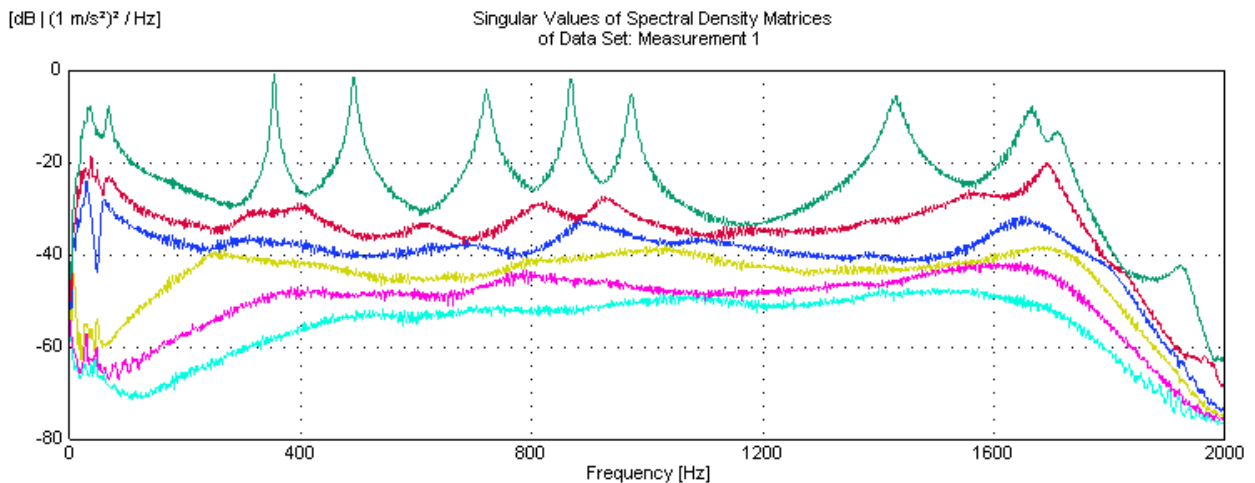


Figure 3. Example with 6 projection channels. The lowest singular value curve is basically horizontal and well attenuated indicating that 6 measurement channels practically contain all the system dynamics.

## 2.2.2 Reducing the Number of Frequencies

The upper curve in a plot of the singular values of the response spectral density matrix will for a structure excited with purely stochastic excitation have peaks at the natural frequencies indicating high singular values. If all the modes are well-separated, there will only be one dominating mode at each peak and consequently the other curves will be significantly lower and less peaked. In case of closely-coupled modes or repeated roots, peaks will appear on the next lower curves as well. The number of curves with significant peaks equals the number of closely-coupled modes or repeated roots. E.g. two modes at the same frequency will result in two large singular values at that frequency.

In case of strong harmonic excitation of the structure, narrow peaks will be found in multiple of the singular value curves at the harmonic excitation frequencies. In Figure 1 the natural frequency of the first bending mode appears at 354 Hz and only the first singular value is significant at this frequency. However, at the deterministic excitation at 374 Hz, 748 Hz (2<sup>nd</sup> harmonic) and 1496 Hz (4<sup>th</sup> harmonic), a distinct narrow peak appears in several of the singular value curves.

If an abrupt change happens at the same frequency in at least two singular value curves, then we have detected a potential harmonic component that should subsequently be tested using the kurtosis check method described in Chapter 2.1. In this way it is possible to significantly reduce the number of frequencies to be checked.

For a matrix  $S$  of positive singular values with dimension  $(n_p, n_s)$  where  $n_p$  is the number of projection channels and  $n_s$  the number of discrete frequencies:

$$S = \begin{bmatrix} S_{11} & \cdots & S_{1n_s} \\ \vdots & & \vdots \\ S_{n_p 1} & \cdots & S_{n_p n_s} \end{bmatrix} \quad (5)$$

we can construct the following normalized matrix  $X$  with dimension  $(n_p, n_s)$ :

$$X = \begin{bmatrix} x_{11} & \cdots & x_{1n_s} \\ \vdots & & \vdots \\ x_{n_p 1} & \cdots & x_{n_p n_s} \end{bmatrix}, \quad x_{i,j} = \begin{cases} \log_{10} \left( \frac{S_{i,j}}{\text{median}(S_{i,j-k}, \dots, S_{i,j+k})} \right) & , j > k \wedge j < n_s - k \\ 0 & , j \leq k \wedge j \geq n_s - k \end{cases} \quad (6)$$

where  $i$  is the singular value index,  $j$  the discrete frequency index and  $k$  is a small number, say 2-5.

If the median of the values  $S_{i,j-k}$  to  $S_{i,j+k}$  is equal to the value  $S_{i,j}$  then  $x_{i,j}$  is 0. Otherwise  $x_{i,j}$  will be a non-zero value. Since the sequence is normalized using the median that is robust towards outliers, the result is that  $x_{i,j}$  will have significant values at indices corresponding to where the singular value curves have significant but narrow peaks.

The method used here is called Fast Kurtosis Checking and contains the following steps:

1. Construct the matrix  $X$  by calculating the elements  $x_{i,j}$  for  $i = 1$  to  $n_p$  and  $j = 1$  to  $n_s$ .
2. Calculate the sampled standard deviations of the  $n_p$  sequences  $\{x_{i,1} \dots x_{i,n_s}\}$ .
3. Check if the  $x_{i,j}$  elements exceed a certain threshold of say 2-3 times the standard deviation.
4. For those indices  $j$ , where more than one of the  $n_p$  sequences  $\{x_{i,1} \dots x_{i,n_s}\}$  exceed the threshold, potential harmonic components have been detected at the  $j$  positions.
5. Apply the kurtosis check method described in Chapter 2.1 at the  $j$  positions.

For the aluminum plate example shown in Figure 1, only the frequencies 28 Hz, 372 Hz, 374 Hz, 376 Hz, 746 Hz, 748 Hz and 1496 Hz were indicated as potential harmonic components. The method consequently resulted in checking only 7 instead of 1024 frequencies. The kurtosis check method from Chapter 2.1 then subsequently identified only the frequencies 374 Hz, 748 Hz and 1496 Hz as harmonic components.

### 3 Removing the Influence of the Harmonic Components

#### 3.1 The Enhanced Frequency Domain Decomposition Technique

The original EFDD technique has been described in a series of papers, see e.g. Gade et al. [4]. The EFDD technique rely on a decomposition of the spectrum of the measured response defined as:

$$G_{yy}(f) = H(f) G_{xx}(f) H^H(f) \quad (7)$$

where  $G_{yy}(f)$ ,  $G_{xx}(f)$  and  $H(f)$  are the spectra of the measured response, the unknown excitation and the Frequency Response Function (FRF), respectively. The key step in the EFDD technique is to perform a Singular Value Decomposition (SVD) of  $G_{yy}(f)$  at the discrete frequencies  $f = f_i$ :

$$G_{yy}(f_i) = U_i S_i U_i^H = \sum_{k=1}^{n_y} u_{ki} u_{ki}^H s_{ki}, \quad n_y: \text{number of measured responses} \quad (8)$$

Assuming no repeated roots, the rank of  $G_{yy}(f_n)$  is approximately 1 at the natural frequency  $f = f_n$ :

$$G_{yy}(f_n) \sim u_{n1} u_{n1}^H s_{n1} \quad (9)$$

This indicates that at the natural frequency the spectrum is approximately equal to the space spanned by the 1<sup>st</sup> singular vector multiplied by the 1<sup>st</sup> singular value. As documented in e.g. Brincker et al. [5] the vector  $u_{n1}$  approximates the mode shape of the mode with natural frequency  $f_n$ .

In the vicinity of the natural frequency the singular vectors have a high MAC value with  $u_{i1}$  enabling us to establish a Single-Degree-Of-Freedom (SDOF) spectral density function  $S(f)$  for the specific mode. This SDOF function is transformed to the time domain yielding an auto-correlation function from where the natural frequency is obtained by determining the number of zero-crossings as a function of time using a simple least-squares fit. The damping ratio is obtained from the logarithmic decrement of the auto-correlation function again using a simple least-squares fit.

#### 3.2 The Curve-Fitting Frequency Domain Decomposition Technique

The Curve-fitting Frequency Domain Decomposition (CFDD) technique is a novel alternative approach utilizing curve-fitting of  $S(f)$  directly in the frequency domain. The main benefit is a more accurate estimation of the natural frequencies and damping ratios in the presence of deterministic excitation (harmonic components). The mode shapes are found as in the original EFDD technique.

In Equation (7) the spectral density was defined in terms of the FRF. The FRF for a SDOF system can be expressed in polynomial form as (see Ljung [6]):

$$H(f) = \frac{B(f)}{A(f)} = \frac{B_0 + B_1 e^{2\pi f T} + B_2 e^{4\pi f T}}{1 + A_1 e^{2\pi f T} + A_2 e^{4\pi f T}}, \quad T: \text{sampling interval} \quad (10)$$

From the roots of  $A(f)$  the natural frequency and the damping ratio can be extracted.

Assuming the unknown excitation  $G_{xx}(f)$  in Equation (7) can be approximated by broad-banded white noise with constant spectrum  $G_{xx}(f) = G_{xx}$ , the SDOF spectrum  $S(f)$  becomes proportional to the product  $H(f)H^H(f)$ , indicating that the polynomial order of  $S(f)$  is twice the order of  $H(f)$ .

To fit  $H(f)$  instead of the product  $H(f)H^H(f)$  the full-power spectrum  $S(f)$  is transformed to a positive half-power spectrum  $P(f)$ .  $P(f)$  is obtained from  $S(f)$  by calculating the respective correlation function obtained by inverse Fourier transformation. The negative lags part of the correlation functions is set to zero and  $P(f)$  is obtained by forward Fourier transformation.

### 3.2.1 The Curve-Fitting Algorithm

The first step of the curve-fitting algorithm is to calculate the positive half-power spectrum  $P(f)$ . Based on this and the formulation of  $H(f)$  in Equation (10) we can set up the following relation:

$$(1 + A_1 e^{2\pi f T} + A_2 e^{4\pi f T})P(f) = B_0 + B_1 e^{2\pi f T} + B_2 e^{4\pi f T} \quad (11)$$

which can be rearranged so the unknown polynomial parameters are isolated:

$$\begin{bmatrix} -P(f) e^{2\pi f T} & -P(f) e^{4\pi f T} & 1 & e^{2\pi f T} & e^{4\pi f T} \end{bmatrix} \begin{bmatrix} A_1 \\ A_2 \\ B_0 \\ B_1 \\ B_2 \end{bmatrix} = P(f) \quad (12)$$

Given the spectral estimates  $P(f_i)$  for all discrete frequencies  $f_i$ ,  $i = 0$  to  $v$ , where  $v$  is the index of the Nyquist frequency, Equation (12) makes it possible to formulate the following regression problem:

$$A_c \theta = B_c, \quad A_c = \begin{bmatrix} -P(f_0) e^{2\pi f_0 T} & -P(f_0) e^{4\pi f_0 T} & 1 & e^{2\pi f_0 T} & e^{4\pi f_0 T} \\ -P(f_1) e^{2\pi f_1 T} & -P(f_1) e^{4\pi f_1 T} & 1 & e^{2\pi f_1 T} & e^{4\pi f_1 T} \\ \cdot & \cdot & \cdot & \cdot & \cdot \\ \cdot & \cdot & \cdot & \cdot & \cdot \\ -P(f_v) e^{2\pi f_v T} & -P(f_v) e^{4\pi f_v T} & 1 & e^{2\pi f_v T} & e^{4\pi f_v T} \end{bmatrix}, \quad B_c = \begin{bmatrix} P(f_0) \\ P(f_1) \\ \cdot \\ \cdot \\ P(f_v) \end{bmatrix}, \quad \theta = \begin{bmatrix} A_1 \\ A_2 \\ B_0 \\ B_1 \\ B_2 \end{bmatrix} \quad (13)$$

To assure that the parameters of  $\theta$  will be estimated as real valued parameters, a regression problem of double size is formulated and a solution using matrix pseudo-inversion is found:

$$\begin{bmatrix} \text{Re}(A_c) \\ \text{Im}(A_c) \end{bmatrix} \theta = \begin{bmatrix} \text{Re}(B_c) \\ \text{Im}(B_c) \end{bmatrix} \quad \Rightarrow \quad \hat{\theta} = \begin{bmatrix} \text{Re}(A_c) \\ \text{Im}(A_c) \end{bmatrix}^{-1} \begin{bmatrix} \text{Re}(B_c) \\ \text{Im}(B_c) \end{bmatrix} \quad (14)$$

The natural frequency and damping estimates are obtained from the roots of  $A(f)$  in (10) and the mode shapes from a weighted sum of singular vectors as in the original EFDD technique.

### 3.2.2 The Curve-Fitting Algorithm in the Presence of Harmonic Components

To apply the curve-fitting algorithm on responses containing harmonic components, the harmonic components first have to be removed. In Jacobsen et al. [2], an approach was used where the removal was done by linear interpolation in the SVD plot. This is shown for the aluminum plate example in Figure 4.

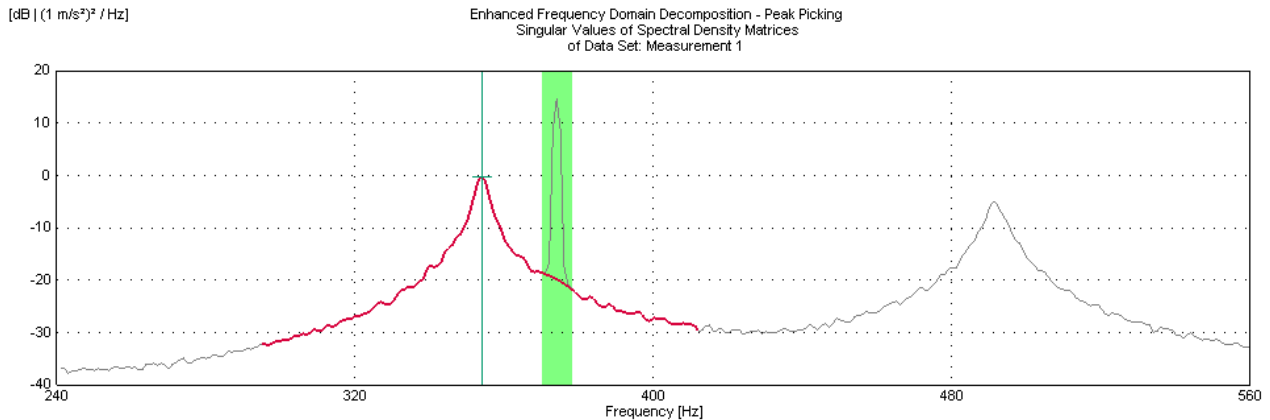


Figure 4. Removal of harmonic component in the SVD plot using linear interpolation. Structural mode at 354 Hz. Harmonic component at 374 Hz.

The method gave good results but the accuracy could be improved when a harmonic component was located exactly at or very close to the natural frequency of a structural mode. In these cases the estimation of the natural frequency would be biased and the damping ratio would be overestimated – the peak of the SDOF function was slightly cut off due to the linear interpolation.

When subsequently curve-fitting is used the limitation of the linear interpolation is less critical. Consequently the linear interpolation method has been applied in the initial implementation of the CFDD technique. However, a least-squares fit approach is currently being investigated, where extrapolation is made from singular values at both sides of the harmonic component.

Figure 5 shows for the aluminum plate example the CFDD curve-fitter on the interpolated SDOF function.

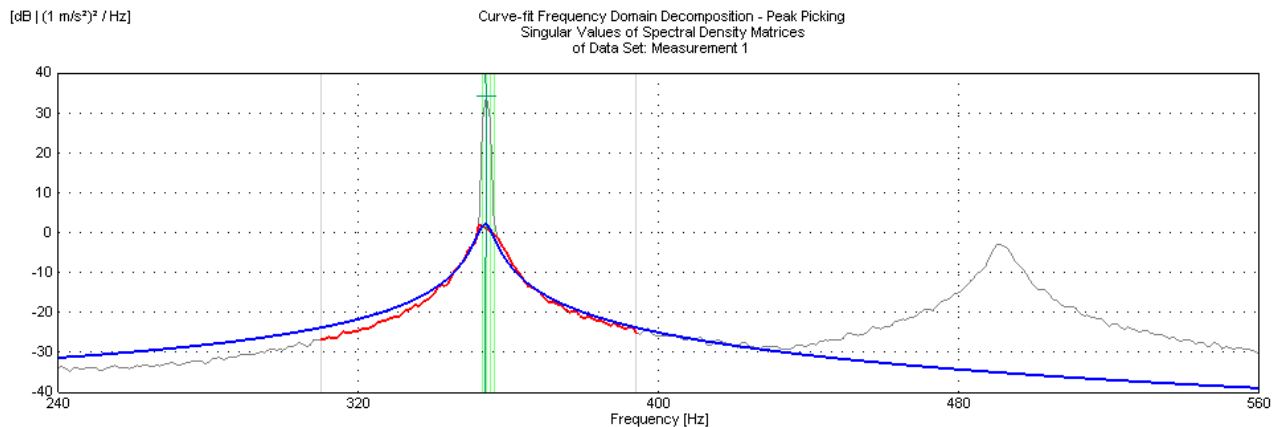


Figure 5. Removal of harmonic component in the SVD plot using first linear interpolation (red graph) and then the CFDD curve-fitter (blue graph). Structural mode and harmonic component both at 354 Hz.

## 4 Applications Examples

The responses of mechanical engineering structures like aircraft, helicopters, vehicles, ships, engines, generators, turbines, compressors, white goods, disk drives, power tools etc. are often quite complex. They are typically a combination of harmonic components originating from the rotating and reciprocating parts and broadband components originating from either self-generated vibrations from, for example, bearings and combustions or from ambient excitations like air turbulence and road vibrations.

Though civil engineering constructions like buildings, towers, bridges and offshore structures are mainly exposed to broadband ambient excitation from wind, waves, traffic or seismic micro-tremors, harmonic excitation from, for example, ventilation systems, turbines and generators are often present as well.

In the following two examples are shown - a ship structure and a gravity dam.

#### 4.1 Ship Structure

In this example, the measurements described in Rosenow et al. [7] are analyzed with the Fast Kurtosis Checking method and the CFDD technique. The measurements were done by Sven-Erik Rosenow, Santiago Uhlenbrock and Günther Schlottmann from University of Rostock, Germany.

The structure, which is shown in Figure 6, is a roll-on roll-off ship from Flensburg shipyard.



Shipyard:  
 Flensburger Schiffbaugesellschaft  
 Length over all: 199,8 m  
 Ship speed: 22,5 kn

**Main engine:**  
 9L 60 MC-C (MAN B&W, 9 cylinder)  
 Power: 20 070 kW  
 Nominal rotation speed: 123 rpm  
 Working process: two-stroke

**Propeller:**  
 4-bladed with controllable pitch

Figure 6. Investigated object, roll-on roll-off ship at the Flensburg shipyard and ship data.

An in-operation test of the ship was carried out in a single data set using 16 channels. The measurement time was 5400 s (90 min) with a sampling frequency of 128 Hz. The number of projection channels was set to 6. The harmonic detection described in Chapter 2.2 was applied using  $k = 2$  in Equation (6). The threshold used in step 3 of the algorithm was set to 2 times the standard deviation of the sequence  $X_{i,j}$ .

In Figure 7 the result of the harmonic detection is shown. The main engine introduces excitation forces into the ship structure at all frequencies that are whole multiples of its rotational frequency (two-stroke engine). In this specific test, the rotational frequency was 2.05 Hz. From the propeller, main excitation forces are transmitted into the ship in form of pressure pulses acting on the ship's hull. The propeller blade frequencies are multiples of 8.20 Hz (4-bladed propeller). All harmonic components at 2.05 Hz interval have clearly been detected. The first harmonic component resulting from the first excitation order of the main engine is very close to the second structural mode.

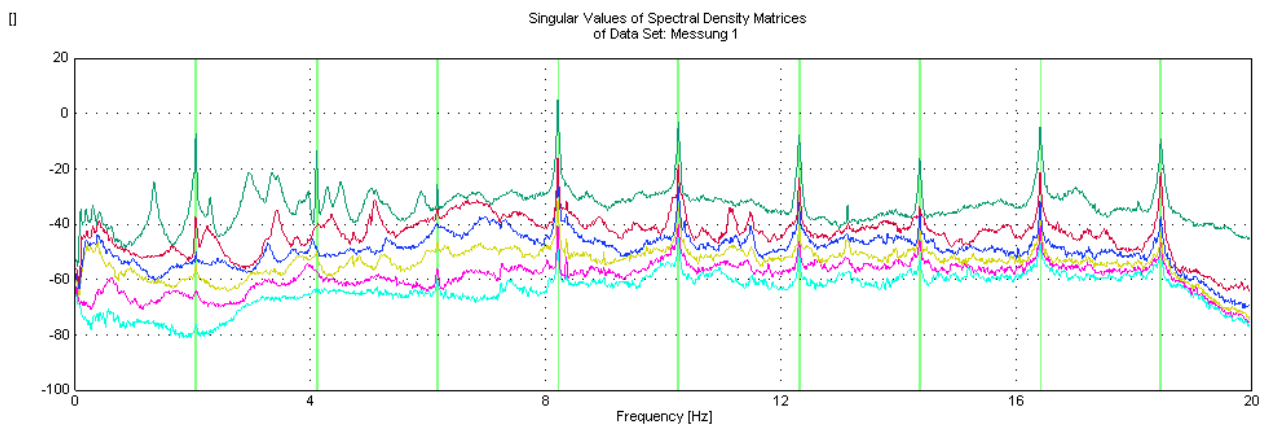


Figure 7. Harmonic components with 2.05 Hz interval are clearly detected.

In Figure 8, the CFDD curve-fitter is shown on the second structural mode after prior linear interpolation in the SDOF function. The harmonic component is clearly eliminated and the second structural mode properly extracted.

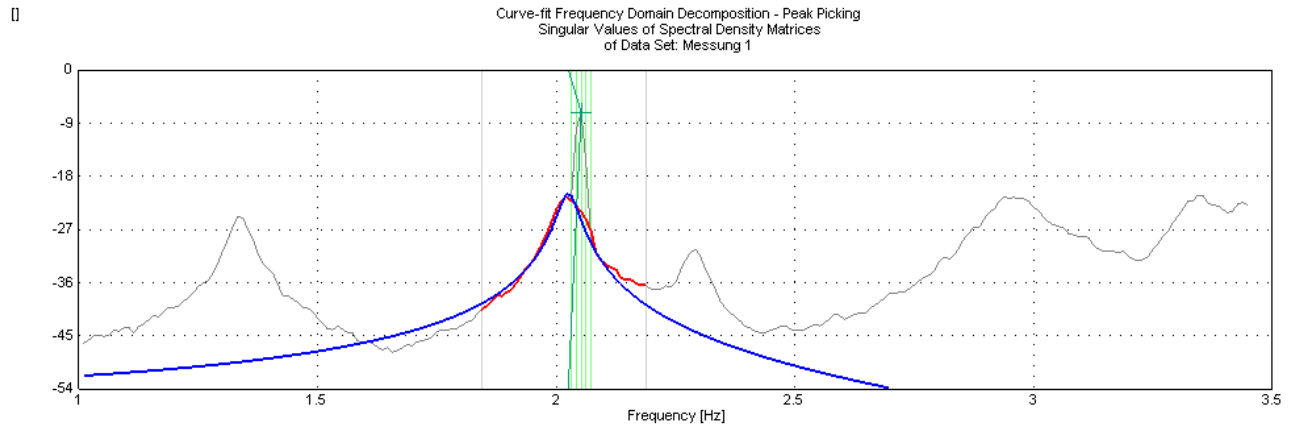


Figure 8. Removal of harmonic component in the SVD plot using first linear interpolation (red graph) and then CFFD curve-fitting (blue graph). Structural mode at 2.03 Hz. Harmonic component at 2.05 Hz.

## 4.2 Gravity Dam

This example is from Andersen et al. [3]. The measurements were done by Carlos Ventura, University of British Columbia, Canada. The structure, which is shown in Figure 9, is a gravity dam of dimensions 58 m high and 130 m long. It was built in 1930.



Figure 9. The gravity dam seen from low (left) and high (right) water levels.

An ambient vibration test was conducted in 20 data sets each with 8 channels. 3 reference DOFs were used. The measurement time was 819 s with a sampling frequency of 80 Hz. As one of the transducers was faulty in one of the data sets, the number of projection channels used in the analysis was set to 7. The harmonic detection described in Chapter 2.2 was applied using  $k = 2$  in Equation (6). The threshold used in step 3 of the algorithm was set to 2 times the standard deviation of the sequence  $X_{ij}$ .

In Figure 10 the result of the harmonic detection is shown. Due to the turbines running, the measurements are affected by harmonic components at every 2 Hz. All harmonic components at 2 Hz interval have been detected. The algorithm has incorrectly detected two harmonic components at 19.5 Hz and 39 Hz, respectively. Taking the scatter of the SVD spectrum from the poor signal-to-noise ratio into account, it is a quite satisfactory result.

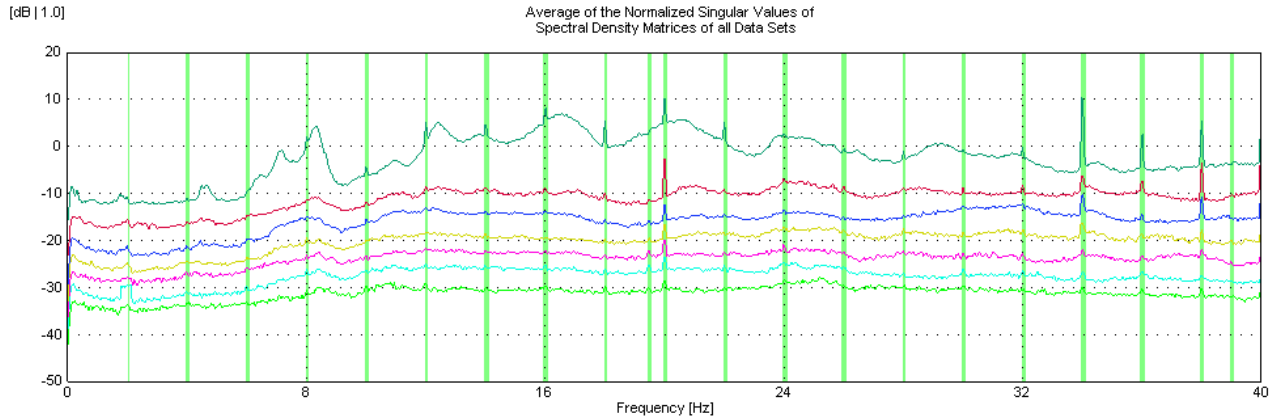


Figure 10. Harmonic components with 2 Hz interval are clearly detected. The algorithm has incorrectly detected harmonic components at 19.5 Hz and 39 Hz due to poor signal-to-noise ratio.

## 5. Other Measurement Considerations

Detection and suppression of harmonic components is vital, when performing Operational Modal Analysis on structures with rotating parts. But other measurement considerations need special attention as well. This includes dynamic range and time recording length considerations.

### 5.1 Dynamic Range

Compared to Classical Modal Analysis using hammer or shaker excitation, the input forces - and hence the output frequencies and levels - can typically not be controlled when performing Operational Modal Analysis. Consequently, a high dynamic range is required to avoid erroneous measurements from overload and underrange situations. In addition, when harmonic components are present, their levels are often much higher than the stochastic broadband excitation from where the modal parameters have to be extracted.

The dynamic range  $DR$  is defined as the ratio between the RMS value of a full-scale sine wave  $V_{FS}$  and the RMS value of the system base noise  $V_N$ . It is typically given in dB:

$$DR = 20 \times \log \frac{V_{FS}}{V_N} \quad (15)$$

When discussing dynamic range, the frequency bandwidth of the measurement must be taken into consideration. In a well-designed system the inherent system noise can be characterised as white noise. Consequently, if all elements of the measurement chain are linear in nature, the dynamic range of the measurement can be improved by reducing the measurement frequency bandwidth. This is actually one of the advantages of the commonly used FFT analysis.

#### 5.1.1 Dynamic Range of Transducers

A high-quality transducer, including preamplifier, can deliver a practically noise-, spurious- and distortion-free signal over a dynamic range of 120 to 130 dB using broadband, and 160 dB using narrowband (effective noise bandwidth 6 Hz), analysis as indicated in Table 1, where 6 Hz corresponds to the effective noise bandwidth of a 25.6 kHz FFT analysis with 6400 lines using Hanning weighting (see Randall [8]).

<b>Bandwidth [Hz]</b>	25.6k	1.024	24	6	1
<b>V<sub>FS</sub> [V<sub>RMS</sub>]</b>	5				
<b>V<sub>N</sub> [V<sub>RMS</sub>]</b>	3μ	600n	92n	46n	19n
<b>DR [dB]</b>	124	138	155	161	169

Table 1. Dynamic ranges for a high-quality transducer in different effective noise bandwidths.

### 5.1.2 Potential Dynamic Range of a Data Acquisition System

For a data acquisition system the theoretical dynamic range in dB, can be calculated as (see Clayton [9]):

$$DR = 20 \times \log \left( 2^N \times \sqrt{\frac{F_S}{2 \times F_{NBW}}} \right) \quad (16)$$

where  $N$  is the system quantization in bits,  $F_S$  the sampling frequency and  $F_{NBW}$  the effective narrowband analysis bandwidth in Hz.

Using Equation (16) Table 2 shows the dynamic range in different bandwidths as a function of system quantization.

N [bits]	Resolution	Dynamic Range				
		F <sub>NBW</sub> [Hz]				
		32.768	1.024	24	6	1
16	65.536	96	111	128	134	141
20	1.048.576	120	135	152	158	166
24	16.777.216	144	160	176	182	190

Table 2. Dynamic ranges for different system quantization and bandwidth.  $F_s = 65.536$  Hz.

Narrowband analysis can improve the analysis depth quite dramatically and an ideal 24-bit system can fully match the performance of modern transducers. In practice, however, most of these ADCs do not have a useful dynamic range higher than 100 – 110 dB due to analysis chain imperfections like harmonic distortion, cross-talk, spurious signals, ADC resolution and non-linearity, aliasing and DSP imperfections. Consequently, high-quality transducers have clearly outperformed analysis systems with respect to dynamic performance – until recently.

### 5.1.3 Dyn-X Technology

With the invention of the Dyn-X technology, data acquisition systems for the first time fully match the dynamic performance of high-quality transducers (see Jacobsen et al. [10]). In brief, the technology utilises a specialised analog input design to provide a very high dynamic range of the analog circuit, pre-conditioning the transducer signal before feeding it to the ADC. The Dyn-X input channels have no input attenuators, but a single input range from 0 to  $10V_{peak}$ . The digitising is performed synchronously in two specially selected, high-quality, 24-bit delta-sigma ADCs, and both data streams are fed to the DSP environment where dedicated algorithms in real-time merge the signals while obtaining an extremely high accuracy match in gain, offset and phase (see Figure 11).

With no setting of input ranges, and with no need to be concerned about overloads, under-range measurements and the accuracy of the measurements obtained, the ease and safety of Operational Modal Analysis measurements are dramatically increased using Dyn-X technology. And with no need for trial runs to ensure correct input ranges for the various input channels, the certainty of getting the measurements right the first time is also significantly increased.

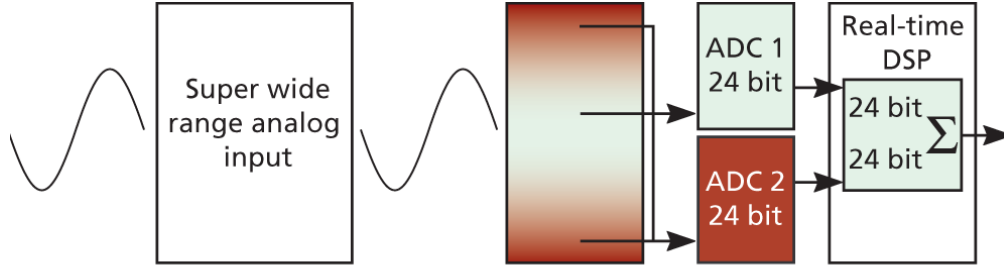


Figure 11. A simplified block diagram of the Dyn-X technology.

## 5.2 Time Recording Length

Another important measurement consideration when performing Operational Modal Analysis measurements is the length of the time recording. In Operational Modal Analysis, data acquisition is done by recording time histories. A pre-requisite for extracting the modal parameters is that all frequencies of interest are sufficiently excited. How long recording time is required depends on various factors such as the spectral shape and duration of the excitation signal, presence of harmonic components, the complexity of the test object and the quality of the data acquisition equipment. However, as a rough rule of thumb, the time histories should at least be 500 times longer than the period of the lowest mode of interest:

$$T_{History} > n / f_{\min} \quad \Lambda \quad n \geq 500 \quad (17)$$

Especially when dominant harmonics are present in the responses and/or the measurements are performed using run-up/down excitation, a long time recording length is required.

For the EFDD and CFDD techniques additional factors must be taken into consideration. The number of statistically independent averages  $n_d$  – corresponding to the so-called BT-product (product of the effective analysis bandwidth  $B$  and the total effective time length  $T_{Total}$ ) – should be sufficient high to minimize errors in the spectral density estimates as explained in Herlufsen [11]. At the same time, the frequency line spacing  $\Delta f$  should be small enough to include a sufficient number of frequency lines  $n_l$  within the 3 dB bandwidth  $B_{3dB}$  of the narrowest SDOF function of interest to be able to accurately estimate the damping.

Using Hanning weighting with an overlap of minimum 50% this can be expressed as:

$$\frac{1}{\sigma_n^2} = n_d \approx 2 \cdot \frac{T_{History}}{T_{Record}} \quad \Lambda \quad \frac{1}{T_{Record}} = \Delta f < \frac{B_{3dB}}{n_l} \quad (18)$$

where  $\sigma_n^2$  is the normalized variance of the spectral estimates,  $T_{History}$  is the length of the complete time history recording and  $T_{Record}$  the length of the FFT records.

Rearranging Equation (18) gives:

$$T_{History} > \frac{n_l}{2 \cdot \sigma_n^2 \cdot B_{3dB}} \quad (19)$$

Equation (19) assumes stochastic broadband responses. When harmonic components are present, the time history length should, in general, be longer.

## 6. Conclusions

Performing Operational Modal Analysis on structures with rotating parts set special demands on the data acquisition and analysis due to the presence of harmonic components. The consequences of harmonic components can be quite drastic and can result in significantly biasing of the modal parameters obtained or even prohibit the extraction of the structural modes.

This paper has described a new method based on the original EFDD technique, where the harmonic components are identified using a Fast Kurtosis Check method and then removed by first performing a linear interpolation across the harmonic components in the SDOF function and secondly applying a curve-fitting using the novel CFDD technique. The method has been demonstrated on measurements from a ship structure and a gravity dam.

This new combined approach offers some distinct benefits:

- Robust method – Harmonic components are clearly identified and their effect can be eliminated even in the case of a harmonic component located exactly at a structural mode.
- No prior knowledge required – For example about the number of harmonic components and their frequencies.
- Ease-of-use – Automated method based on the CFDD technique.
- Fast – Based on computational efficient algorithms using Fast Kurtosis Checking.

As the output levels can typically not be controlled in Operational Modal Analysis measurements, a high dynamic range is required to eliminate overload and underrange situations and to account for the high signal levels in dominant harmonic components. With the invention of the Dyn-X technology, the data acquisition system for the first time fully match the dynamic performance of high-quality transducers thereby making Operational Modal Analysis measurements safe, easy and accurate - even in the presence of strong harmonic components.

Finally considerations about time recording length were discussed and rules of thumb were given. Again the presence of harmonic components set additional demands on the time recording length.

## Acknowledgments

The authors would like to thank Sven-Erik Rosenow, Santiago Uhlenbrock and Günther Schlottmann, University of Rostock, Germany for providing the measurement data of the roll-on roll-off ship from Flensburg shipyard and Carlos Ventura, University of British Columbia, Canada for providing the measurement data of the Canadian gravity dam.

## References

- [1] N-J. Jacobsen, *Separating Structural Modes and Harmonic Components in Operational Modal Analysis*, IMAC XXIV Conference, 2006
- [2] N-J. Jacobsen, P. Andersen, R. Brincker, *Eliminating the Influence of Harmonic Components in Operational Modal Analysis*, IMAC XXV Conference, 2007
- [3] P. Andersen, R. Brincker, C. Ventura, R. Cantieni, *Estimating Modal Parameters of Civil Engineering Structures subject to Ambient and Harmonic Excitation*, EVACES'07 Conference, 2007
- [4] S. Gade, N. Møller, H. Herlufsen, H. Konstantin-Hansen, *Frequency Domain Techniques for Operational Modal Analysis*, 1<sup>st</sup> IOMAC Conference, 2005
- [5] R. Brincker, L. Zhang, P. Andersen, *Output-Only Modal Analysis by Frequency Domain Decomposition*, ISMA25 Conference, 2000
- [6] L. Ljung, *System Identification – Theory for the User*, 2<sup>nd</sup> Edition, Prentice Hall, Upper Saddle River, N.J., 1999
- [7] S-E. Rosenow, S. Uhlenbrock, G. Schlottmann, *Parameter Extraction of Ship Structures in Presence of Stochastic and Harmonic Excitations*, 2<sup>nd</sup> IOMAC Conference, 2007
- [8] R. B. Randall, *Frequency Analysis*, Brüel & Kjær, 3<sup>rd</sup> edition, 1987
- [9] G. B. Clayton, *Data Converters*, MacMillan Publishers, 1<sup>st</sup> edition, 1982
- [10] N-J. Jacobsen, O. Thorhauge, *Dyn-X Technology, Order Tracking, Comparison of IBEM, PNAH and LDV Methods*, Brüel & Kjær Technical Review No.1, 2006, BV0058-11
- [11] H. Herlufsen, *Dual Channel FFT Analysis (Part II)*, Brüel & Kjær Technical Review No.2, 1984, BV0014-11